The Influence of The Pro-inflammatory Cytokine, Osteopontin, On Autoimmune Demyelinating Disease

Dorothée Chabas*[1], Sergio E. Baranzini*[2], Dennis Mitchell[1], Claude C.A. Bernard[3], Susan R. Rittling[4], David T. Denhardt[4], Raymond A. Sobel[5], Christopher Lock[1], Marcela Karpuj[1,2], Rosetta Pedotti[1], Renu Heller[6], Jorge R. Oksenberg[2]-, and Lawrence Steinman[1,7]-

*both authors contributed equally to the work

-both senior authors contributed equally

[1] Dept. of Neurology and Neurological Sciences, Beckman Center for Molecular Medicine, B002, Stanford, CA 94305

[2] Department of Neurology, University of California at San Francisco School of Medicine, San Francisco, CA 94143

[3] Neuroimmunology Laboratory, Department of Biochemistry, La Trobe University, Bundoora, Victoria, 3083 Australia

[4] Department of Cell Biology and Neuroscience, Rutgers University, Piscataway, NJ 08854

[5]Dept. of Pathology {Neuropathology}, Stanford University School of Medicine, Stanford CA 94305

[6] Roche Bioscience, 3401 Hillview Avenue, Palo Alto CA 94304

[7]To whom editorial correspondence should be addressed: email steinman@stanford.edu

Multiple sclerosis is a demyelinating disease, characterized by inflammation in the brain and spinal cord, possibly due to autoimmunity. Large scale sequencing of cDNA libraries, derived from plaques dissected from brains of patients with multiple sclerosis [MS], indicated an abundance of transcripts for osteopontin. Microarray analysis of spinal cords from rats paralyzed from experimental autoimmune encephalomyelitis [EAE], a model of MS, also revealed increased OPN transcripts. Osteopontin deficient mice were resistant to progressive EAE and had frequent remissions, and myelin-reactive T cells in OPN-/- mice produced more IL-10 and less g-interferon than in +/+ mice. Osteopontin thus appears to regulate Th1 mediated demyelinating disease, and may offer a potential target in blocking development of progressive MS.

Multiple sclerosis [MS] is often characterized by relapsing episodes of neurologic impairment followed by remissions. In about a third of MS patients this disease evolves into a progressive course, termed secondary progressive MS (1). In a minority of patients progressive neurologic deterioration without remission occurs from the onset of disease, and this is called primary progressive MS. The pathophysiologic and genetic causes underlying primary versus secondary progressive MS remain unclear (2, 3, 4).

Osteopontin, also called early T cell activation gene-1, (5, 6), has pleiotropic functions (7, 8, 9), including roles in inflammation and in immunity to infectious diseases (8). OPN costimulates T cell proliferation (8), and is classified as a Th1 cytokine, due to its ability to enhance IFN-gamma and IL-12 production, and to diminish IL-10 (10). We investigated a role for OPN in MS and an experimental model for MS, experimental autoimmune encephalomyelitis [EAE].

Initially we set out to identify gene transcripts involved in the inflammatory response that might be increased in the central nervous system during active EAE, and which returned to normal when EAE was successfully treated after the onset of paralysis. Customized oligonucleotide microarrays were produced to monitor transcription of genes involved in inflammatory responses (11-14). These initial microarray experiments showed that osteopontin transcripts were elevated in the brains of rats with EAE, and not in brains of rats protected from EAE. Details of these experiments are available on the internet (14).

In parallel, we performed high throughput sequencing of expressed sequence tags [EST], utilizing non-normalized cDNA brain libraries (15, 16, 17), generated from MS brain lesions and control brain (18). Using this protocol the mRNA populations present in the brain specimens are accurately represented, enabling the quantitative estimation of transcripts and comparisons between specimens (18) (Table 1 and web Table 1 [ref. 14]). Molecular mining of two sequenced libraries and their comparison with a normal brain library, matched for size and

tissue type, and constructed with an identical protocol, revealed that OPN transcripts were frequently detected, and exclusive to the MS mRNA population, but not that of control brain (Table 1).

We sequenced over 11,000 clones from MS libraries 1 and 2, and control libraries, respectively (Web Fig. 1 [ref. 14]), and focused analysis on genes present in both MS libraries, but absent in the control library (18). This yielded 423 genes, including 26 novel genes. From those, 54 genes showed a mean fold change of 2.5 or higher in MS libraries 1 and 2 [Table 1]. Transcripts for alpha B-crystallin, an inducible heat shock protein, localized in the myelin sheath, and known to be targeted by T cells in MS, were the most abundant transcripts unique to MS plaques (19) [Table 1]. The next five most abundant transcripts, included those for prostaglandin D synthase, prostatic binding protein, ribosomal protein L17, and OPN.

Next we analyzed all genes present in each of the three cDNA libraries, and found 330 (7 novel) genes. Based on the clone count of each sequenced gene, a table was constructed with transcripts showing an average fold difference [AFD] equal or greater than ±2.00 between MS and control. Forty of these transcripts were divided into three levels, based on the consistency of differential expression across libraries (web table 1 [ref. 14]). Some of these genes (web Table 1 [ref. 14]), included myelin basic protein [MBP], heat shock protein 70 [HSP-70], glial fibrillary acidic protein [GFAP] and synaptobrevin. MBP transcripts displayed consistent high levels of expression in the 3 libraries, suggesting a very high turnover rate for this protein. Expression of HSP70-1, which is involved in myelin folding (20) was significantly elevated. Although not differentially expressed, GFAP was among the three most abundant species in all the libraries, consistent with a prominent glial (or astrocytic) response in the MS brains. Six genes belonging to the KIAA group of large-size cloned mRNAs, showed differential expression. The decreased transcription of synaptobrevin might be of interest given that it belongs to a family of small integral membrane proteins specific for synaptic vesicles in neurons. Recent evidence indicates that axonal loss is one of the major components of pathology in MS (21, 22).

Given the known inflammatory role for OPN, we examined the cellular expression pattern of this protein in human MS plaques and in control tissue, by immunohistochemistry. To identify cells expressing OPN *in situ* we used a polyclonal antibody, generated in mouse against recombinant GST-OPN, to stain postmortem MS and control tissue samples (23) (Fig. 1A and B). Within active MS plaques OPN was found on microvascular endothelial cells and macrophages (Fig. 1A), and in white matter adjacent to plaques. Reactive astrocytes and microglia also expressed OPN (Fig. 1B).

The role of OPN in inflammatory demyelinating disease was next examined using two models of EAE (1). A relapsing-remitting model of EAE was first used to compare the cellular expression of OPN at different stages of the disease. Disease was induced in SJL mice by immunization with the peptide PLP139-151 in complete Freund's adjuvant [CFA], and the animals were scored daily for signs of disease (24). Brain and spinal cord were removed either during acute phase, remission or first relapse (25). Histopathologic identification of OPN in EAE was then performed. (Fig. 1C-F). OPN was expressed broadly in microglia during both relapse and remission from disease, and this expression was focused near perivascular inflammatory lesions. In addition to OPN expression on glia, expression in neurons was detectable during acute disease, and relapse, but not during remission. To confirm the expression of OPN in an acute form of EAE, a rapid, monophasic demyelinating disease was induced in Lewis rats (12), and OPN immunostaining was performed on brains (Fig. 1G) (29). OPN expression in microglia and neurons was predominant in the sick rats, and was focused close to the acute lesions, as was observed in the relapsing/remitting mouse model of EAE. Staining of OPN in bone with the same antibody MPIIIB10_1 served as a positive control (Fig. 1H). These results strongly implicated OPN in acute, as well as in relapsing forms of EAE, and suggested that the degree of expression of OPN in lesions correlated with the severity of disease.

The potential role of OPN in demyelinating disease was next tested using OPN deficient mice [Fig. 2](30). EAE was induced using MOG 35-55 in CFA in OPN-/- mice and OPN+/+ controls (31). EAE was observed in 100% of both OPN+/+ and OPN-/- mice with MOG 35-

55. Despite this, severity of disease was singificantly reduced in all animals in the OPN-/- group (Fig. 2A), and these mice were totally protected from EAE-related death (Fig. 2B). Thus, OPN significantly influenced the course of progressive EAE induced by MOG 35-55.

The rate of relapses and remissions was next tested. During the first 26 days, OPN-/- mice displayed a distinct evolution of EAE, with a much higher percentage of mice having remissions compared to the controls (Fig. 2C). OPN+/+ and OPN-/- mice were sacrificed on days 28, 48, and 72 post-immunization for histopathology. Although the clinical courses in the two groups were quite different, there were similar numbers and appearances of inflammatory foci within the central nervous system (32). Therefore, although OPN may not influence the extent of the inflammatory response, this molecule might critically influence whether or not the course of disease is progressive, or whether relapses and remissions develop.

To examine whether different immune responses were involved in OPN-/- and OPN+/+ animals, we tested the profile of cytokine expression in these mice. Since EAE is a T cell mediated disease, we first analyzed the T cell proliferative response to the auto-antigen MOG 35-55 in the OPN-/- mice. T cells in OPN-/- mice showed a reduced proliferative response to MOG 35-55, compared with OPN+/+ T cells (Fig. 3A). In addition, IL-10 production was increased in T cells reactive to MOG 35-55 in OPN-/- mice that had developed EAE, compared with T cells in OPN+/+ mice (Fig. 3B). At the same time, IFN-gamma and IL-12 production was diminished in the cultures of spleen cells stimulated with MOG (Fig. 3C-D).

Since IFN-γ and IL-12 are important pro-inflammatory cytokines in MS (1, 33), the finding that in OPN-/- mice there is reduced production of these cytokines, is consistent with the hypothesis that OPN may play a critical role in the modulation of Th1 immune responses in MS and EAE. Further, IL-10 has been associated with remission from EAE (34). In this context, the enhancement of myelin specific IL-10 production in OPN-/- mice, may account for the tendency of these mice to go into remission. Sustained expression of IL-10 may thus be an important factor in the reversal of relapsing MS, and its absence may allow the development of secondary progressive MS.

In conclusion our data support the idea that OPN may have pleiotropic functions in the pathogenesis of demyelinating disease. OPN production by glial cells may lead to the attraction of Th1 T cells, and its presence in glial and ependymal cells may allow inflammatory T cells to penetrate the brain. Finally, our data suggest that neurons may also secrete this proinflammatory molecule and participate in the autoimmune process. Potentially, neuronal OPN secretion could modulate inflammation and demyelination, and influence the clinical severity of the disease. Consistent with this idea, a role for neurons in the pathophysiology of MS and EAE has recently been described (21,22), and neurons are known to be capable of cytokine production (35,36). OPN inhibits cell lysis (6), and thus neuronal OPN might even protect the axon from degeneration during autoimmune demyelination.

CD44 is a known ligand of OPN, mediating a decrease of IL-10 production (10). As shown here, OPN-/- mice produced elevated IL-10 during the course of EAE. We recently demonstrated that anti-CD44 antibodies prevented EAE (37), suggesting that the proinflammatory effect of OPN in MS and EAE might be mediated by CD44. The binding of OPN to its integrin fibronectin receptor $\alpha_V \beta_3$ through the arginine-glycine-aspartate tripeptide motif may also perpetuate Th1 inflammation (10). In active MS lesions, the α_V subunit of this receptor is overexpressed in macrophages and endothelial cells, and the β_3 subunit is expressed on endothelial cell luminal surfaces (23). Via its tripeptide binding motif, OPN inhibits inducible nitric oxide synthetase (iNOs) (38), which is known to participate in autoimmune demyelination (1). Thus in conclusion, OPN is situated at a number of checkpoints that would allow diverse activities in the course of autoimmune mediated demyelination.

References and Notes

1. L. Steinman, *Nature **Immunology** 2*, 762 (2001*)*.

2. J. L. Haines et al., *Nat Genet* **13**, 469 (1996).

3. G. C. Ebers et al., *Nat Genet* **13**, 472 (1996).

4. S. Sawcer et al., *Nat Genet* **13**, 464 (1996).

5. A. Oldberg, A. Franzen, D. Heinegard, *Proc Natl Acad Sci U S A* **83**, 8819 (1986).

6. L. W. Fisher, et al., *Biochem Biophys Res Commun* **280**, 460 (2001).

7. D. T. Denhardt, X. Guo, *Faseb J* **7**, 1475 (1993).

8. A. W. O'Regan et al., *Immunol Today* **21**, 475 (2000).

9. S. R. Rittling, D. T. Denhardt, *Exp Nephrol* **7**, 103 (1999).

10. S. Ashkar et al., *Science* **287**, 860 (2000).

11. The custom microarray has 517 genes, with 60 probe pairs per gene, and a feature size of 50X50 micrometers. Rat, mouse and human genes for cytokines, chemokines, bone growth factors, proteases, and molecules related to cell death are included on this chip.

12. N. Karin et al., *J Immunol* **160**, 5188 (1998).

13. K. Gijbels, R. E. Galardy, L. Steinman, *J Clin Invest* **94**, 2177 (1994).

14. Rats were treated with 75 mg/kg/day orally of the MMP inhibitor RS110379, from day 10- day 16, and sacrificed on day 16. Further information on this experiment, as well as details of the analysis of transcripts with custom microarrays, and Web Figure 1 and Web Table 1, appear as supplementary information on the internet at Science Online {www.sciencemag.org/xxx}..

15. K. G. Becker et al., *J Neuroimmunol* **77**, 27 (1997).

16. S. S. Choi et al., *Mamm Genome* **6**, 653 (1995).

17. N. Sasaki et al., *Genomics* **49**, 167 (1998).

18. In contrast to normalized libraries in which high frequency transcripts are preferentially eliminated by nuclease treatment of DNA/RNA hybrids to facilitate detection of rare RNA species, we produced non-normalized libraries, where manipulation of clones is avoided. White matter brain tissue from the plaques of 3 MS patients was collected and frozen within two hours after death. Patient history on the specimen used for the first library (herein MS1) included clinically definite MS, and the presence of active inflammatory lesions. Material for the second MS library (herein MS2) came from a pool of tissues from two patients, one with acute, active lesions and widespread inflammatory involvement in the white matter, and the other with chronic, "silent" lesions, with gliosis, but without evidence of a lymphocytic infiltrate. The control library (CTRL) was constructed using pooled mRNA isolated from midbrain white matter, inferior temporal cortex, medulla, and posterior parietal cortex tissue removed from a 35-year-old Caucasian male who died from cardiac failure and who had no neuropathological changes. Details of construction of the libraries can be found on the internet at Science Online {www.sciencemag.org/xxx}, particularly in the legends to Web Fig. 1 and web Table 1[ref. 14].

19. J. M. van Noort et al., *Nature* **375**, 798 (1995).

20. D. A. Aquino et al., *Neurochem Res* **23**, 413 (1998).

21. D. Pitt, P. Werner, C. S. Raine, *Nat Med* **6**, 67 (2000).

22. B. D. Trapp et al., *N Engl J Med* **338**, 278 (1998).

23. R. A. Sobel et al., *J Neuropathol Exp Neurol* **54**, 202 (1995).

24. R. Pedotti et al., *Nat Immunol* **2**, 216 (2001).

25. Mice were sacrificed during relapse and remission and perfused with 60ml of 10% formalin. Brain and spinal cord were removed and fixed in the same solution. 6-10 micron paraffin sections were prepared. OPN was detected with the monoclonal anti-OPN antibody MPIIIB10_1 (Developmental Studies Hybridoma bank, Iowa City, IA), at 1/50 dilution, using the Vector® M.O.M. immunodetection kit (Vector Laboratories, cat# PK 2200), the Vectastain® Elite ABC kit (Vector Laboratories, cat# PK 6100) according to the manufacturer's instructions, and the substrate D.A.B. (0.5mg/ml for 4 minutes). The intensity of the cellular staining was evaluated by a blind observer according to a semiquantitative scale (3 grades). MPIIIB10_1 stains OPN in immunohistochemical sections from mice, though it does not recognize OPN on Western blots (26). The successful use of MPIIIB10_1 in mouse sections has been reported (27,28).

26. S. R. Rittling, F. Feng, *Biochem Biophys Res Commun* **250**, 287 (1998).

27. N.Dorheim et al J Cell Phys **154,** 317 (1993).

28. C. Grainger Nature Med **1,**1063 (1995).

29. Details of immunohistochemical staining were performed as described in Supplementary material (14).

30. S. R. Rittling, et al., *J Bone Miner Res* **13**, 1101 (1998).

31. A. Slavin et al., *Autoimmunity* **28**, 109 (1998).

32. OPN+/+ and OPN-/- mice are 129/C57Bl/6 mixed background, maintained as a partially outbred strain (30). Induction of EAE is described further as supplementary information on the Internet.

33. L. Steinman, *Cell* **85**, 299 (1996).

34. M. K. Kennedy et al., *J Immunol* **149**, 2496 (1992).

35. H. Villarroya et al., *J Neurosci Res* **49**, 592 (1997).

36. S. L. Shin et al., *Neurosci Lett* **273**, 73 (1999).

37. S. Brocke et al., *Proc Natl Acad Sci U S A* **96**, 6896 (1999).

38. S. M. Hwang et al., *J Biol Chem* **269**, 711 (1994).

39. P. J. Ruiz et al., *J Immunol* **162**, 3336 (1999).

40. High throughput EST sequencing was performed in collaboration with Incyte Geneomics. We thank Beatrice Romagnolo for her outstanding help when setting up the breeding of the mice and her statistical expertise and Jane Eaton for her technical support. We thank the NIH, the NMSS, the Susan G Komen Foundation, the Association Française Contre Les Myopathies, the Ligue Française Contre La Sclérose En Plaques, and the Assistance Publique des Hopitaux de Paris for support.

Table 1: MS-Specific Gene Transcripts.

Only genes with a mean fold change of >2.5 are listed. N/A, mapping position is not known. *, genomic regions that reached nominal criteria of linkage in genome-wide screenings.

Accession #	Gene description	MS1 abundance	MS2 abundance	Average clone count	Cellular function	Genomic location
S45630	Alpha B-crystallin	7	12	9.5	cell structure/motility	11q22.3-q23.1
M61901	Prostaglandin D synthase	8	7	7.5	cell signalling/ cell communication	9q34.2-34.3
X75252	Prostatic binding protein	6	7	6.5	cell signalling/ cell communication	12q24.1 *
X53777	Ribosomal protein L17	10	2	6	gene/protein expression	18q
X13694	***Osteopontin***	***8***	***3***	***5.5***	***cell structure/motility/signaling***	***4q21-q25***
AB037797	KIAA1376	6	3	4.5	unclassified	5
Z19554	Vimentin	4	5	4.5	cell structure/motility	10p13
X52947	Cardiac gap junction protein	5	3	4	cell signalling/ cell communication	6q21-q23.2 *
D17554	DNA-binding protein	4	4	4	gene/protein expression	12q23-24.1 *
AF181862	G protein-coupled receptor	2	6	4	cell signalling/ cell communication	16p12
AB018321	ATPase, Na/K transporting, alpha 2 (KIAA0778)	2	6	4	cell signalling/ cell communication	1q21-q23
AF100620	MORF-related gene X	1	7	4	gene/protein expression	Xq22 *
AB002363	KIAA0365	1	7	4	unclassified	19p12
AF072902	Gp130 associated protein GAM	6	1	3.5	unclassified	19p13.3
M11233	Cathepsin D	6	1	3.5	cell/organism defense	11p15.5
D78014	Dihydropyrimidinase related protein-3	6	1	3.5	metabolism	5q32
X53305	Stathmin	4	3	3.5	cell division	1p36.1-p35 *
AF026844	Ribosomal protein L41	4	3	3.5	unclassified	22q12
U48437	Human amyloid precursor-like protein 1	4	3	3.5	unclassified	N/A
U51678	Small acidic protein	3	4	3.5	unclassified	N/A
U67171	Selenoprotein W	3	4	3.5	metabolism	19q13.3 *
S80794	Tyrosine and tryptophan hydroxylase activator	2	5	3.5	cell signalling/ cell communication	22q12.3
AB011089	KIAA0517 (brain)	4	2	3	unclassified	4q28
AAD32952	PHR1 isoform 4 [Mus musculus]	3	3	3	unclassified	N/A
J04173	Phosphoglycerate mutase, brain	2	4	3	metabolism	10q25.3
M22382	Heat shock 60kD protein 1 (chaperonin)	2	4	3	cell/organism defense	2
M34671	HUMCD59A Human lymphocytic antigen CD59/MEM43	2	4	3	unclassified	11p13
M64786	Similar to Myc	2	4	3	unclassified	N/A
AJ132695	Rac1 gene	2	4	3	cell signalling/ cell communication	Xq26.2-27.2
Z99716	Septin 3	1	5	3	cell division	22q13.1
U49436	Human translation initiation factor 5	1	5	3	gene/protein expression	14q32 *
CAA63354	Cysteine string protein [Bos taurus]	2	3	2.5	unclassified	N/A
U90915	Cytochrome c oxidase subunit IV	4	1	2.5	metabolism	16q24.1
J02611	Apolipoprotein D	4	1	2.5	metabolism	3q26.2-qter
X05607	Cystatin C (cysteine proteinase inhibitor precursor)	4	1	2.5	metabolism	20p11.2
U45976	Clathrin assembly protein lymphoid myeloid leukemia	4	1	2.5	unclassified	11q14
J00272	Metallothionein-II pseudogene	4	1	2.5	unclassified	4p11-q21
S69965	Beta-synuclein	3	2	2.5	unclassified	5q35
Y00711	Lactate dehydrogenase B	3	2	2.5	metabolism	12p12.2-p12.1
L37033	FK-506 binding protein homologue (FKBP38)	3	2	2.5	cell signalling/ cell communication	19p12
AF044956	NADH:ubiquinone oxidoreductase B22 subunit	3	2	2.5	metabolism	8q13.3
AB011154	KIAA0582 (brain)	3	2	2.5	unclassified	2p12
X55039	Centromere autoantigen B	3	2	2.5	unclassified	20p13
X64364	Basigin	3	2	2.5	cell signalling/ cell communication	19p13.3
U82761	S-adenosyl homocysteine hydrolase-like 1	3	2	2.5	metabolism	1
D13627	Chaperonin containing TCP1, subunit 8 (theta)	2	3	2.5	gene/protein expression	21q22.11
Z47087	Transcription elongation factor B (SIII), polypeptide 1-lik	2	3	2.5	gene/protein expression	5q31
X75861	Testis enhaced gene transcript	2	3	2.5	cell division	12q12-q13
M16447	Quinoid dihydropteridine reductase	2	3	2.5	metabolism	4p15.31
M22918	Non-muscle myosin alkali light chain	2	3	2.5	unclassified	12
M55270	Matrix Gla protein	2	3	2.5	unclassified	12p13.1-p12.3
AF151807	CGI-49 protein	2	3	2.5	unclassified	1
AAD45960	Human EST H08032.1 (NID:g872854)	2	3	2.5	unclassified	7q11.23-q21.1

Figure 1

CNS expression of osteopontin in demyelinating disease

A,B. MS. OPN in macrophages in the center of an actively demyelinating MS plaque (A) and in white matter astrocytes adjacent to an active MS plaque (B). OPN staining was performed with a polyclonal anti-OPN antibody on paraffin-embedded sections.

C-F. Relapsing-remitting EAE in mice. EAE was induced in nine SJL mice (The Jackson Laboratory, Bar Harbor, ME) with PLP 139-151, as previously described (24). Four mice injected with PBS served as controls. Immunostaining was performed with the anti-OPN antibody MPIIIB10_1 (Developmental Studies Hybridoma bank, Iowa City, IA) (25) and slides were examined by a blinded observer. (C) OPN was broadly expressed in CNS microglia, especially near inflammatory lesions, but not in adjacent peripheral nerves (arrow). (D) Expression in neurons (arrows) was detectable during the acute phase (N=4) and relapse (N=2), but not during remission (N=1) or in mice with inflammatory lesions which never developed paralysis (N=2). (E) OPN expression in astrocytes (arrows) and choroid plexus cells (F) was also more frequent and more pronounced in immunized mice (100%) than in controls (25%).

G. Acute EAE in rat. EAE was induced in 19 Lewis rats (The Jackson Laboratory) as described in (13) but with 400 μg GPSCH. Four rats injected with CFA alone served as controls. Brains were processed and stained with MPIIIB10_1 (29). Microglial expression of OPN around inflammatory lesions (G) correlated with the clinical disease severity. OPN was also expressed in neurons (arrows), mostly in the animals with severe clinical signs.

H. Positive control. OPN staining in the bony growth plate of a mouse femur with MPIIIB10$_1$.

All photos are immunoperoxidase stained with diaminobenzidine chromogen and hematoxylin counterstain. Magnifications: A-D, F, H = 370X; E,G = 494X.

Figure 2

Clinical attenuation of EAE in OPN-/- mice

EAE was induced in OPN+/+ (N=18) [closed circles] and OPN-/- (N=17) [open circles] mice (30) with MOG 35-55, as described in (31). EAE was scored as followed: 0: normal - 1:monoparesis - 2: paraparesis – 3: paraplegia – 4: Tetraparesis – 5: moribund or dead. For each animal a remission was defined by a decrease of the score of at least one point for at least two consecutive days. EAE was considered remitting when at least one remission occurred within the 26 first days, and progressive when no remission occurred.

(A): OPN-/-[open circles] mice have milder disease than OPN+/+ controls [closed circles]. The error bars represent the standard error for each point. EAE was observed in 100% of both OPN+/+ and OPN-/- mice with MOG 35-55, [N=18 for OPN+/+ and N=17 for OPN-/-]. Although EAE could be induced with a 100% incidence in OPN-/- mice, a significantly reduced severity of disease developed in the OPN-/- group, with a decrease of the mean EAE score (at day 30, mean EAE score 2.5 in OPN+/+, compared to 1.2 in OPN-/-, Mann-Whitney Rank Sum test p=0.0373) and a decrease of the mean maximum severity score (mean severity 3.7 in OPN+/+, compared to 2.8 in OPN-/-, Mann-Whitney Rank Sum test p=0.0422) . There was no significant delay of the day of onset of disease (mean 11.7 days in OPN+/+, compared to 12.5 days in OPN-/-, Mann-Whitney Rank Sum test p=0.322). **(B)**: OPN-/- mice (open

circles) are protected from EAE related death, zero dead out of 17, cmpared to 7 dead out of 18 in the OPN+/+ mice at day 70 (p=0.0076 by Fisher's exact test). **(C)**: OPN promotes progressive EAE. The bars represent the percentage of mice having a remitting (black) or progressive (white) disease in each group. OPN-/- mice showed a distinct evolution of EAE, with a much higher percentage of mice having remissions compared to the controls. (10 out of 18 had remissions in the OPN+/+ group (55.5%), compared to 16 out of 17 in the OPN-/- group (94.1%), p = 0.0178 by Fisher's exact test).

Figure 3

Attenuated T cell activation by MOG35-55 in OPN-/- mice

(A): Inhibition of T cell proliferation in OPN-/- mice. A proliferation assay was performed on draining lymph nodes [LN] from OPN+/+ (closed circles) and OPN-/- (open circles) mice (30), 14 days after induction of EAE. EAE was induced with MOG 35-55, as described in (31). Draining LN were removed 14 days after immunization, and LN cells were stimulated in 96-well flat bottom plates (2.5 10^6/ml, 200µl/well) with serial dilutions of HPLC purified MOG 35-55 (0-50µM), as described (39). The medium contained 2% serum from the type of mouse tested, in order to avoid introducing OPN into the in vitro assays on OPN-/- cells: OPN+/+ normal mouse serum was used for the assays on OPN+/+ cells, while OPN-/- normal mouse serum was used for the assays on OPN-/- cells**.** Concanvalin A (2µg/ml), a non-specific mitogen for T cells, was used as a non specific positive control. [^{3}H] thymidine was added to the triplicates [mean $\pm$ standard deviation graphed], after 72h of antigen stimulation and its incorporation by the proliferating cells (in cpm) was measured 24h later. **(B)**: **OPN -/- cells produce more IL-10 than OPN+/+ cells**. OPN+/+ (black bars) and OPN-/- (white bars)

LN cells were stimulated in the same way as for the proliferation assay (Fig. 3A), but in 24-well flat bottom plates (2ml/well). MOG 35-55 was used at a concentration of 12.5µM. IL-10 was measured by ELISA on the 48h supernatants (dilution 1/2), in duplicate [mean ± standard deviation graphed], according to the manufacturer's instructions.

Fig 3C: **OPN-/- cells produce less IFN-gamma than OPN+/+ cells**. OPN+/+ (filled bars) and OPN-/- (open bars) spleen cells were removed 14 days after induction of EAE with MOG 35-55 and stimulated as described for Fig. 3B, but with 4.5 10^6 cells/well. IFN-gamma was measured by ELISA on the 48h supernatants (dilution 1/5), in triplicate[1], according to the manufacturer's instructions. **(D): OPN-/- cells produce less IL-12 than OPN+/+ cells**. OPN+/+ (black bars) and OPN-/- (white bars) spleen cells were removed as described for Fig. 3C. IL-12 p70 was measured by ELISA on the 24h supernatants (dilution 1/1), in duplicate [mean ± standard deviation graphed], according to the manufacturer's instructions (OPTEIA kit, PharMingen, San Diego, CA).

Fig. 1

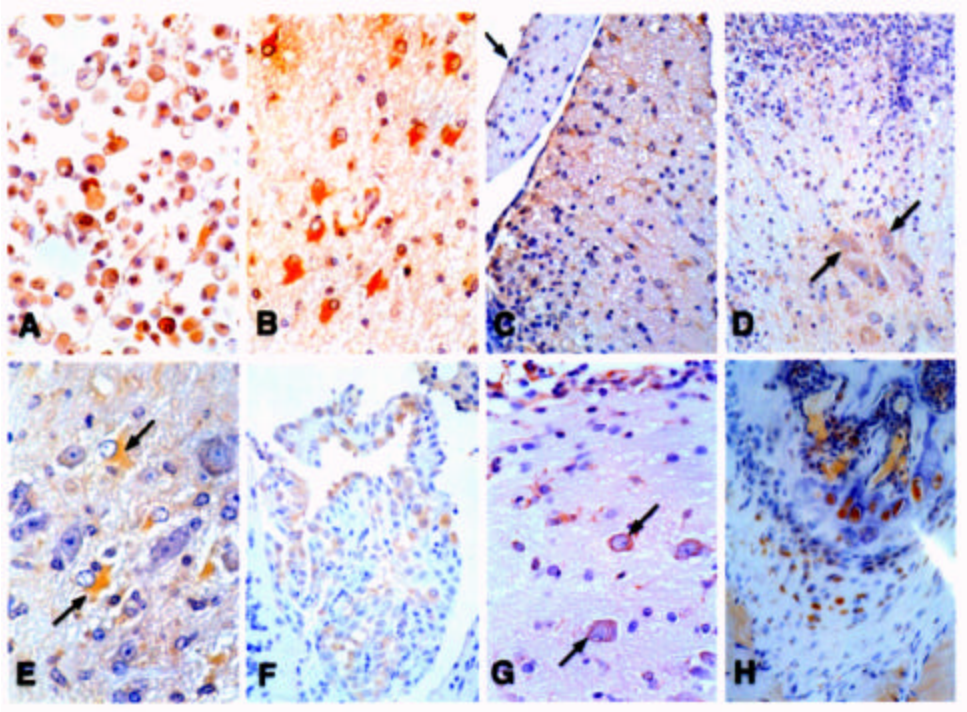

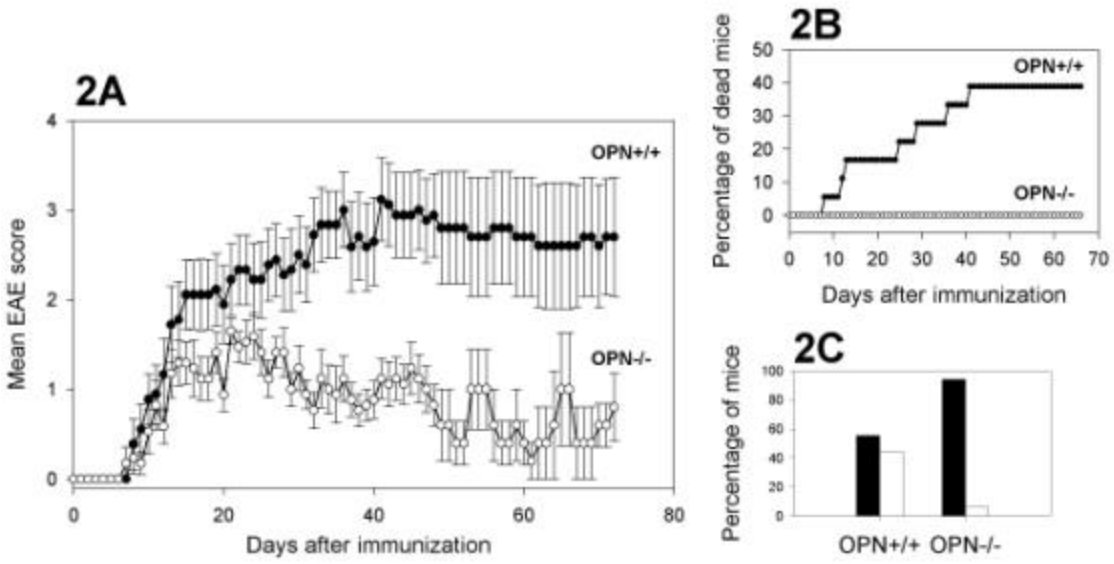
2A
Mean EAE score
Days after immunization
OPN+/+
OPN-/-
2B
Percentage of dead mice
Days after immunization
OPN+/+
OPN-/-
2C
Percentage of mice
OPN+/+ OPN-/-

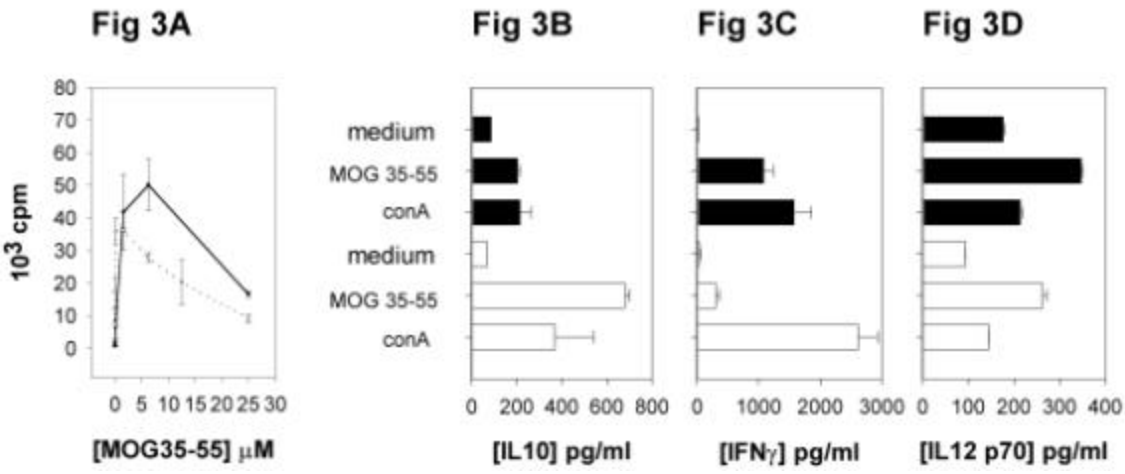
Fig 3A
Fig 3B
Fig 3C
Fig 3D
10^{-3} cpm
80
70
60
50
40
30
20
10
0
0 5 10 15 20 25 30
[MOG35-55] μM
medium
MOG 35-55
conA
medium
MOG 35-55
conA
0 200 400 600 800
[IL10] pg/ml
0 1000 2000 3000
[IFNγ] pg/ml
0 100 200 300 400
[IL12 p70] pg/ml

Supplementary Material

Web Table 1, Available on the Internet. Genes differentially expressed in MS and normal libraries^

^ Only genes corresponding to transcripts with an average fold difference of ≥2 are listed. The first section of the table lists genes whose expression was statistically significant in both MS libraries when compared to the CTRL library (Fisher's exact test, $p<0.05$). The second section contains genes with significant difference in expression in only one of the MS libraries and the CTRL. The last section includes genes with non-significant differences but AFD ≥ ±3.00. N/A, mapping position is not known. *, genomic regions that reached nominal criteria of linkage in genome-wide screenings.

Accession #	Gene description	Clone count			Average	Cellular function	Genomic location
		MS1	MS2	CTRL	Fold-difference		
M17885	Acidic ribosomal phosphoprotein P0	9	13	2	5.2	gene/protein expression	12q24 *
X16869	Elongation factor 1-alpha	32	33	15	2.07	gene/protein expression	6q14
M54927	Myelin proteolipid protein	41	16	64	-3	cell structure/motility	Xq22 *
U66623	Small GTPase	1	1	7	-7.35	cell signaling/cell communication	2q21.2
M26252	Piruvate kinase, muscle	2	1	10	-8.04	Energy metabolism	15q22
M59828	Heat shock protein 70-1	2	14	1	7.29	cell/organism defense	6p21.3 *
AF068846	Scaffold attachement factor A	6	1	1	2.49	Cell division	N/A
AF035283	Clone 23916	10	15	5	2.36	unclassified	N/A
U46571	Tetratricopeptide repeat protein 2	10	4	3	2.29	unclassified	17q11.2
AF131756	clone 24912	2	10	10	-3.02	unclassified	N/A
X92845	N-myc downstream regulated	1	7	7	-4	unclassified	8q24.1
M97168	X (inactive)-specific transcript	1	13	10	-4.33	unclassified	Xq13.2
AB023167	Neural membrane protein 35 (KIAA0950)	1	3	7	-4.74	unclassified	12q13
AB002391	HERC2 (KIAA0393)	2	1	7	-5.63	unclassified	15q13
AF055026	RaP2 interacting protein 8	1	1	6	-6.3	Unclassified	17
U89330	Microtubule-associated protein 2	1	1	6	-6.3	cell structure/motility	2q34-q35
M20020	Ribosomal protein S6	5	6	1	5.23	gene/protein expression	9p21 *
X03747	Na/K-ATPase beta subunit	5	5	1	4.78	Energy metabolism	1q22-q25
V00572	Phosphoglycerate kinase	5	4	1	4.33	metabolism	Xq13
M59488	S100 protein beta-subunit	5	4	1	4.33	cell signaling/cell communication	21q22.3
AB018271	KIAA0728 (Brain)	4	4	1	3.83	Unclassified	6p11-11.2
AB020718	KIAA0911	4	3	1	3.38	unclassified	1p36 *
AAD02202	CaM-KII inhibitory protein [Rattus norvegicus]	2	5	1	3.26	unclassified	N/A
D67025	Proteasome 26S subunit (non-ATPase, 3)	1	1	3	-3.15	cell/organism defense	17q21.1
D63424	Glycogen synthase kinase 3 alpha	1	1	3	-3.15	metabolism	19q13.3-13 *
AF051976	Unconventional myosin XV	1	1	3	-3.15	cell structure/motility	17p11.2
X13916	LDL-receptor related protein	1	1	3	-3.15	metabolism	12q13.q14
AB028981	KIAA1058	1	1	3	-3.15	unclassified	13
AF102846	N-ethylmaleimide-sensitive factor	3	1	5	-3.61	metabolism	17q21
L10284	Calnexin	3	1	5	-3.61	cell/organism defense	5q35
D88435	Cyclin G associated kinase	1	2	5	-3.85	cell division	4p16
AF054987	aldolase C	2	1	5	-4.02	metabolism	17cen-q12
CAB01750	similar to Mitochondrial carrier proteins [Caenorhabditis elegans]	1	1	4	-4.2	Unclassified	N/A
AL137406	Clone DKFZp434M162	1	1	4	-4.2	Unclassified	N/A
AB032436	Brain specific Na+-dependent inorganic phosphate cotransporter	1	1	4	-4.2	metabolism	19q13 *
L10911	Splicing factor (CC1.3)	1	1	4	-4.2	gene/protein expression	20
L77864	Amyloid beta (A4) precursor protein-binding, family B, member 1 (Fe65)	1	4	7	-4.42	unclassified	11p15
U64520	Synaptobrevin-3	1	1	5	-5.25	unclassified	1p35-p36
D87465	KIAA0275 (brain)	1	1	5	-5.25	unclassified	10

Web Figure 1 [Supplementary Data]:

Web Fig 1A. Frequency distribution of Libraries. The libraries were made in collaboration with Incyte Genomics. Libraries were constructed using 1.5 mg of polyA RNA from each sample. cDNA synthesis was initiated using a NotI-anchored oligo(dT) primer. Double-stranded cDNA was blunted, ligated to EcoRI adaptors, digested with NotI, size-selected, and cloned into the NotI and EcoRI sites of the pINCY vector (Incyte, Palo Alto, CA). Approximately 4,000 clones from each library were sequenced in ABI automatic DNA Sequencer (Applied Biosciences, Foster City, CA). Annotated data was extracted from the Incyte database LifeSeq Gold® and incorporated into MS Access 2000® and MS Excel 2000® for further analysis. All queries were designed and performed in MS Access, while charts and tables were generated with MS Excel. Cellular roles were assigned after consulting the Expressed Gene Anatomy Database (EGAD, The Institute for Genomic Research, www.tigr.org/egad). Genomic location was included according to NCBI's MapView and Genemap'98. (National Institute for Biotechnology Information, www.ncbi.nlm.nih.gov) Comparisons of gene frequencies between each MS library and the CTRL were performed and the average fold change calculated. Differences in gene expression were subjected to Fisher's exact test and a P-value of 0.05 or lower, was selected as criteria for inclusion in each comparison.

We sequenced 3678, 4174, and 3740 clones from MS1, MS2, and control libraries, respectively . Each of the libraries had a substantial number of clones with no match to the

Genbank database, and were thus considered novel. Clones in library MS1 could be assigned to 2387 different cDNA species from which 331 corresponded to novel genes. MS2 and CTRL yielded 2727 (546 novel) and 2352 (511 novel) species respectively. Analysis of frequency distribution revealed a similar pattern for all three libraries, with the most abundant transcripts being represented by few species including two myelin genes, myelin basic protein, [MBP], and proteolipid protein, [PLP], and the astrocyte-specific transcript, glial fibrillary acidic protein, [GFAP]. Similarly, there was an exponentially decreasing frequency observed for less frequent cDNA species in all three libraries. Taken together the data reveal that the composition and complexity of the three libraries were similar, and that there were no obvious biases, therefore enabling comparative analysis.

Clones with a count higher than 6 were organized in decreasing order according to their frequency. Arrows indicate the three most common ESTs in each library. MBP was the most highly expressed gene in all three libraries. GFAP and PLP were the next most abundant species in the MS libraries, but their frequency order was reversed in the control library. Unidentified ESTs are shown in lighter color than known, annotated clones.

Supplementary Fig 1B. Category distribution. Clones were distributed into one of the following categories: RN, redundant novel; RK, redundant known; HA, high abundance; SN, solitary novel; and SK, solitary known. The relative contribution to each category is shown in a pie chart for all libraries.

Supplementary Fig 1C. Intersectional queries. All possible comparisons were performed among the three libraries. Clones were counted and distributed into their corresponding

intersection on the Venn diagrams. The total number of sequenced clones is shown for each library. The number of different mRNA species for each library is also shown along with the number of unknown genes in parentheses. The number of RNA species that were specific for each library or intersection of libraries is displayed underlined, along with the number of unknown genes in parentheses.

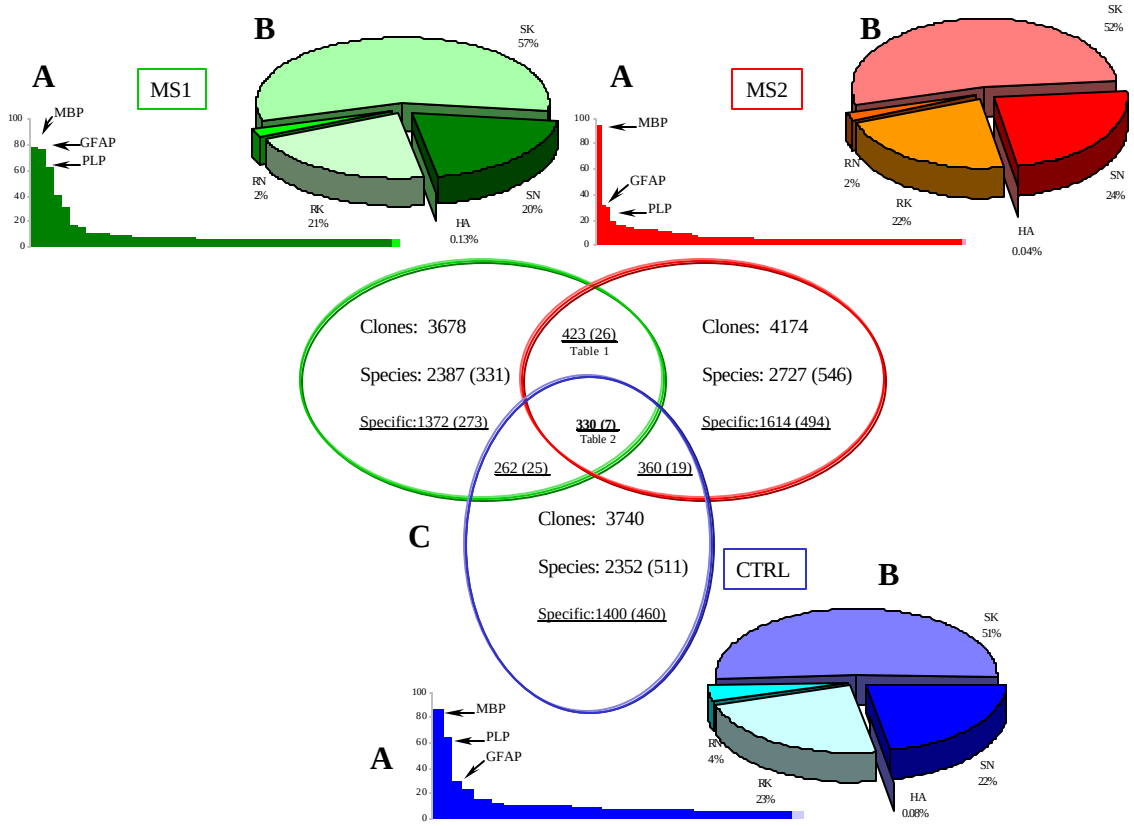

Further supplementary material, Methods and Experimental Details:

Details of immunohistochemical staining: After perfusion with 100ml of 10% formalin, brains were removed at seven different time points between day 11 and day 28 post immunization. OPN was detected with the anti-OPN antibody MPIIIB10_1, dilution 1/50. We used the secondary biotinylated rat adsorbed Anti-Mouse IgG (H + L) antibody from Vector Laboratories (cat# BA 2001)**.** The staining was evaluated by a blind observer according to a semiquantitative scale (3 grades).

Details of Induction of EAE: We induced EAE with MOG 35-55 in CFA in 129/C57Bl/6 OPN-/- mice, and 129/C57Bl/6 OPN+/+ controls. Here we slightly modified the protocol: we injected 100μg of MOG 35-55 emulsion subcutaneously in the flanks of each female at day 0, and 400 ng of Pertussis Toxin at day 0 and day 2.

Seven OPN+/+ and 6 OPN-/- mice were examined on days 28,48 and 72 post immunization for histopathology. Data are unpublished showing similar numbers and appearances of inflammatory foci within the central nervous system in the two groups.

Details of the transcriptional profiling with custom microarrays: Spinal cord was homogenized in TRIzol reagent (Gibco BRL) using a Polytron (Kinematica AG, Switzerland) and total RNA prepared according to the recommended protocol. mRNA was purified by two rounds of selection using oligo(dT) resin (Oligotex, Qiagen). 2 μg of mRNA was used to prepare double stranded cDNA (Superscript, Gibco BRL). The primer for cDNA synthesis contained a T7 RNA polymerase promoter site. 1 μg of cDNA was used for an in-vitro

transcription reaction (Ambion T7 Megascript) with biotinylated CTP and UTP (Enzo Diagnostics, Inc.). The labeling procedure amplifies the mRNA population ~60-fold. Microarray chips (GeneChip™ System, Affymetrix) were hybridized for 16 hours in a 45°C incubator with constant rotation at 60 rpm. Chips were washed and stained on a fluidics station, and scanned using a laser confocal microscope. Affymetrix provided the procedures for sample preparation, fluidics station, scanner, and computer workstation. Chips were analysed with GeneChip v3.1 software, and scaled to a value of 150. The software determines whether a particular RNA transcript is present or absent, based on the intensity of the signal. Fold change was calculated by divided the intensity of the average difference change in the experimental sample by the intensity of the average difference change in the control.

Further details of the initial experiment with custom microarrays (11):

Custom microarrays were designed that allow large scale profiling of mRNA for 517 components of the inflammatory response, including cytokines, chemokines, various adhesion molecules, and matrix metalloproteases. Profiles of mRNA transcripts from the spinal cord of six Lewis rats with EAE were analyzed. Rats were immunized with 400µg of guinea pig spinal cord homogenate [GPSCH] and monitored for EAE as previously described (12). mRNA was isolated from the brain and spinal cord of three rats with hind limb paralysis (mean EAE score 2.7, indicating severe paraplegia), 15 days after immunization with GPSCH, and from three rats treated with a metalloprotease inhibitor after the initiation of EAE. It is established that matrix metalloprotease inhibitors can reverse EAE (13), and rats treated with the metalloprotease inhibitor [RS110379] displayed no clinical disease (mean EAE score 0.2). Spinal cord from two other normal rats served as controls.

OPN transcripts were increased 3.4 fold in the spinal cord of rats with EAE and paralysis, compared to controls without EAE (average difference change for intensity of OPN

transcripts was 16609 fluorescent units in untreated rats with EAE versus an average difference change for intensity in OPN transcripts of 4846 in rats without EAE) (14). After treatment with RS110379, levels of OPN mRNA were no different than control rats without EAE. Thus, there was a 1.1 fold change between the intensity of OPN transcripts in EAE rats treated with MMP inhibitor versus rats without EAE (the average difference of the change in intensity of OPN transcripts on the custom microarrays was 5176 units in rats treated with RS110379 versus an average difference intensity of 4846 units in rats without EAE) (14).